Classical and Quantum Simulations of Tryptophan in Solution

Thomas Simonson,*,† Chung F. Wong,*,‡ and Axel T. Brünger§

Laboratoire de Biologie Structurale (C.N.R.S.), I.G.B.M.C., 1 rue Laurent Fries, 67404 Illkirch (C.U. de Strasbourg), France, Department of Physiology and Biophysics, Mount Sinai School of Medicine, Box 1218, New York, New York 10029-6574, and Howard Hughes Medical Institute, and Department of Molecular Biophysics and Biochemistry, Yale University, 260 Whitney Avenue, New Haven, Connecticut 06511

We use path integral molecular dynamics to study the effect of nuclear tunneling on the structure, fluctuations, and energetics of tryptophan in water. Tryptophan is important as a spectroscopic probe; it can also serve as a miniature model of a protein, possessing charged, polar, hydrophobic, and aromatic groups, hard and soft degrees of freedom, and conformational heterogeneity around its dihedral angles. At room temperature, nuclear tunneling increases the fluctuations of hard internal degrees of freedom by a factor of approximately 2; dihedral fluctuations are not affected. Water structure is weakened, and the solvation energies of the amino, carboxyl, and indole groups change by 1−2 kcal/mol. Solvation energies and free energies of the 1La and 1Lb excited states were analyzed, using semiempirical and ab initio atomic charges, and a free energy perturbation approach. The dielectric relaxation free energy, from Marcus theory, is $1/2$ of the dielectric relaxation energy, for a wide class of systems; this is used to relate the free energy results to experimental Stokes shifts. CNDO/S charges, with the classical ground state simulations, predict a 5.5 kcal/mol red shift for 1La, a large solvent broadening and Stokes shift, in approximate agreement with experimental data for methylindole, with a smaller red shift, solvent broadening, and relaxation for 1Lb. Nuclear tunneling increases the red shift, decreases the solvent broadening, and decreases the solvent dielectric relaxation by 20−30%, consistent with the weaker solvent structure seen in the quantum simulations.

1. Introduction

Nuclear tunneling is known to play a role in the dynamics and function of several biological molecules, affecting ligand binding in heme proteins, electron transfer reactions, and enzymatic proton transfer.[1−3] Path integral simulation techniques provide an increasingly viable approach to study these effects.[4,5] Recent applications to complex systems include studies of liquid water,[6,7] solid and liquid neon,[8−10] buckeyballs,[11] ions in aqueous clusters and bulk water,[12−15] and electron transfer at a metal−water interface.[16] These studies all address equilibrium properties, since ordinary path integral simulations do not allow one to study dynamics in real time. Very recent studies based on the centroid molecular dynamics method of Voth and co-workers[17] are beginning to explore actual quantum dynamics.[18]

Path integral simulations may eventually have applications in other areas, such as simulated annealing and structure refinement, due to the enhanced conformational sampling of the multicopy model. Indeed, semiclassical, Gaussian wave-packet dynamics have been used recently in a simulated annealing procedure to find the global energy minimum of van der Waals and water clusters very efficiently.[19] An analogous procedure could possibly be implemented with path integral dynamics. Multicopy methods have been used recently in crystallographic structure refinement with a great deal of success.[20,21]

Preliminary path integral simulations of the electron transfer protein cytochrome *c* were carried out several years ago,[22,23] demonstrating noticeable quantum effects on the equilibrium fluctuations of the hard internal degrees of freedom even at room temperature. The magnitude of quantum effects on the soft dihedral degrees of freedom was difficult to assess from these simulations, because of the short simulation time (a few tens of picoseconds). Also the convergence of the results with respect to the quality of the path integral represenation (the number of quasiparticles, or "beads", used per atom) was not investigated.

In this article, we report path integral simulations of a simpler biological molecule, tryptophan, in aqueous solution, in order to investigate the magnitude of quantum effects on both the hard and the soft dihedral degrees of freedom, as well as the convergence with respect to simulation length and number of beads. Indeed, tryptophan has in miniature something of the complexity of a real protein: charged, polar, hydrophobic, and aromatic groups; both hard and soft degrees of freedom; and conformational heterogeneity around its dihedral angles.

Tryptophan is also of considerable interest as a spectroscopic probe in proteins. It can potentially be used as a microscopic window into the static and time-dependent dielectric properties of proteins, which are quite difficult to study, both experimentally[24,25] and theoretically.[26−28] Yet, despite a considerable amount of experimental and theoretical work, its spectroscopic properties are still not fully understood. Classical molecular dynamics simulations have been performed on tryptophan,[29] as well as indole and methylindole,[30−32] and various spectroscopic properties calculated. However, the presence of two low-lying excited states, of conformational heterogeneity, the possible formation of specific excited state−solvent complexes (exciplexes), and the rapid time scale of solvent relaxation all complicate studies of this apparently simple molecule. We therefore also report calculations of spectroscopic properties, including the solvent broadening of the excitation energy distributions, and the magnitude of the Stokes shift, and we assess the importance of quantum effects on these properties. We recall that the Stokes shift can be related in a rigorous way

---

* Corresponding authors.
† CNRS.
‡ Mt. Sinai School of Medicine.
§ Yale University.

1936 *J. Phys. Chem. A, Vol. 101, No. 10, 1997*

Simonson et al.

TABLE 1: Ground and Excited State Charges[a]

| | | CNDO/S | | 3-21G | |
| | | ground → 1La[b] | ground → 1Lb | ground → 1La | ground → 1Lb |
atom[c]	ground				
HT1	0.480	0.000	0.000	0.017	0.016
HT2	0.480	0.000	0.000	−0.013	−0.014
N	−0.870	0.001	0.001	0.004	0.004
HT3	0.480	0.000	0.000	−0.013	−0.014
C	0.870	0.000	0.000	−0.013	−0.001
OT1	−0.800	0.002	0.001	−0.013	0.049
OT2	−0.800	0.000	0.000	0.003	0.001
CA	−0.170	0.012	0.007	−0.005	−0.005
HA	0.270	0.001	0.000	0.000	0.001
CB	−0.490	0.014	0.006	−0.008	0.002
HB1	0.270	0.009	0.004	−0.001	−0.007
HB2	0.270	0.002	0.001	0.008	0.009
CG	−0.180	0.159	0.086	0.072	0.034
CD2	−0.110	−0.158	0.020	−0.005	0.023
CD1	0.040	0.112	0.024	−0.005	−0.041
HD1	0.260	0.001	0.000	0.003	0.002
NE1	−0.650	0.117	0.024	0.032	0.038
HE1	0.440	0.000	0.000	0.008	0.006
CE2	0.200	0.028	−0.076	0.015	0.014
CE3	−0.240	−0.081	−0.083	0.062	−0.056
HE3	0.260	0.000	0.000	−0.015	−0.011
CZ2	−0.280	−0.091	−0.044	−0.043	−0.030
HZ2	0.250	0.000	0.000	−0.008	−0.008
CZ3	−0.270	0.042	−0.012	0.009	0.067
HZ3	0.250	0.000	0.000	−0.007	−0.006
CH2	−0.240	−0.172	0.043	0.007	−0.028
HH2	0.250	0.000	0.000	−0.009	−0.008

[a] Charges in atomic units from 3-21G calculation. [b] Charge shifts upon going from ground to 1La excited state from semi-empirical CNDO/S calculation. [c] See atom labels, Figure 4.

through Marcus theory not only to the solvent relaxation energy but also to the solvent relaxation free energy in response to excitation—an occasionally neglected result.[28,33,34]

The next section describes technical details of the classical and quantum molecular dynamics simulations. Path integral molecular dynamics are used to explore equilibrium properties only: quantum dynamics are beyond the scope of this study. Results are presented in the third section; the final section is a discussion. An Appendix recalls the relation between the relaxation energy and free energy in response to a set of perturbing charges.

2. Methods

2.1. Partial Charges and Force Field. Partial charges for tryptophan in its ground and first two excited states were obtained from both ab initio and semiempirical calculations.[35] The 3-21G basis set was used in the ab initio calculations, and the charges were obtained from natural orbital population analyses. The excited state charges were obtained from configuration interaction calculations, which included only single excitations. The calculations were carried out for three stable conformations of the ground state tryptophan, corresponding to the three χ_1 rotamers. The charges were quite similar for the three conformations. Therefore, the averages of these charges were used (Table 1) in the work presented here. Atomic charges obtained from Mulliken and natural orbital population analyses with several basis sets are quite similar. The ab initio ground state charges were used in all the simulations.

Semiempirical Mulliken charges for the ground and excited states were also obtained with the CNDO/S method, for both tryptophan and 3-methylindole, using a program by J. Reimers (University Sydney).[36] These atomic charges reproduce accurately the quantum mechanical dipole moments. The ground → 1La charge shifts from this method were in reasonable

agreement with the INDO/S methylindole charges of Muino and Callis.[32] More importantly, they also led to good agreement for the solvent contribution to the ground → 1La excitation energy and free energy, calculated with the Muino and Callis charges. Below, we analyze the solvent contribution to the 1La and 1Lb excitation energies and free energies using both the ab initio charges and the CNDO/S charges. Since these properties only depend on the charge shifts between ground and excited state, it is permissible to use the CNDO/S charge shifts in combination with simulations done with ab initio charges. Indeed, the solvent contribution to the excitation energy V is given by $V = \sum_i \delta q_i V_i$, where δq_i is the charge shift on atom i upon excitation, and V_i is the solvent electrostatic potential on atom i.

The semiempirical charge shifts will be seen below to give much better agreement with experimental data for indoles. This is probably due to the low level of the ab initio calculations, *i.e.*, to the neglect of electron correlation effects, and the lack of polarization functions in the basis set. These limitations especially affect the excited state charge distribution; they should be much less serious for the ground state. Despite them, we shall report results for quantum effects calculated with both the semiempirical and the 3-21G charge shifts, in order to assess the sensitivity of the quantum effects to the exact partial charge model.

The tryptophan bonded and van der Waals interactions were described by the Amber all-atom force field.[37] Water molecules were described by a modified version of the SPC water model, including intramolecular flexibility.[38] This model has the advantage of a very simple functional form, since intramolecular flexibility is described by harmonic bond stretching and bending terms. Van der Waals interactions between water and tryptophan were treated with the Lorentz−Berthelot combination rules.[37]

This force field was used without any reparametrization in the quantum simulations. Therefore, quantum effects are effectively included in the model twice, since the classical force field is parametrized to include quantum effects implicitly. We disregard this problem here, since the primary purpose of our quantum simulations is to evaluate the effects of quantization by direct comparison to classical simulations performed in the same conditions. In addition, the SPC water model does appear to perform well in path integral simulations.[7,16]

2.2. Molecular Dynamics Simulations. Molecular dynamics simulations were done with periodic boundary conditions, including one tryptophan and 197 water molecules in a cubic cell of edge length 18.836 Å. Long-range interactions were shifted to zero at 9 Å separations, with an atom-based, minimum image convention. The use of a cutoff represents a serious limitation.[39−41] However, as the classical and quantum simulations were carried out in the same conditions, we expect that direct comparison between the two sets of simulations will give a reasonable estimate of the magnitude of quantum effects, despite this simple cutoff treatment.

Langevin dynamics were performed, in which all atoms are subjected to weak friction and stochastic forces, representing thermal coupling to a solvent bath at 293 K. The equations of motion were integrated with a time step of 0.4 fs, which led to very good energy conservation in microcanonical classical and quantum simulations of tryptophan in vacuum. No attempt was made to increase the efficiency by using a multiple time step algorithm to accommodate the high-frequency bond vibrations for example. The list of nonbonded interactions was updated whenever any atom had moved 0.25 Å since the previous update.

Quantum simulations were run in the same conditions, using

either 5 or 10 beads per atom. For details of the path integral simulation method, readers are referred to *e.g.* ref 5.

Classical and quantum simulations were also carried out with the Verlet algorithm (i.e., without friction and stochastic forces) for comparison. In this case, the system was maintained at 293 K by the temperature coupling method of Berendsen et al.,[42] which involves weak velocity scaling.

Simulations were initiated with tryptophan in the (*gauche*[+], *perp*) conformation ($\chi_1 \sim +60°$, $\chi_2 \sim +90°$), and this conformation was retained throughout all the simulations. Experimentally, the *gauche*[−] state is favored in solution,[43] with the *gauche*[+] about 0.5 kcal/mol less stable, and the *trans* about 1 kcal/mol higher. However, the *gauche*[+] state is favored for tryptophan residues in peptides and proteins.[44]

Preparation of the simulations involved extensive equilibration of the classical system with Verlet dynamics, followed by data collection using both Verlet dynamics (600 ps) and Langevin dynamics (200 ps). The classical system served to initiate equilibration and production of the 5-bead quantum system with Verlet dynamics (700 ps); Langevin dynamics were started from the end of the quantum Verlet simulation and run for 400 ps. Simulation of the 10-bead quantum system was started from the end of this last run; the starting bead velocities were modified by adding a random component, drawn from a Maxwellian distribution at 20 K. Langevin dynamics were run for 250 ps, and the last 200 were ps used for analysis. Results are reported from the Langevin dynamics runs unless otherwise noted.

Calculations were carried out with the program X-PLOR,[45] using only standard features. This program has a general facility for limiting atomic interactions to specific subsystems in a very flexible way (the so-called "constraints interaction" statement). Thus the quantum simulations use multiple copies of each atom (multiple beads), linked by harmonic springs to form atomic necklaces. Interactions between beads (other than the harmonic springs) are limited to beads of the same rank in different necklaces. Harmonic springs between successive beads in each necklace are implemented in X-PLOR as pseudo-NOE restraints. X-PLOR script files are available from the authors.

2.3. Excitation Free Energies and Dielectric Relaxation. We calculate the solvent contribution to the excitation free energies for the 1La and 1Lb excited states using thermodynamic perturbation theory.[46,47] The shifts in the atomic partial charges upon excitation are obtained from both ab initio and semiempirical calculations. We calculate only the contribution of tryptophan−solvent interactions to the excitation energy and free energy. The contribution from intramolecular interactions is not expected to be accurately described by a simple, classical, atomic partial charge model. The solvent contribution to the excitation free energy ΔF, for a particular excited state, is given by the perturbation formula

$$\Delta F = -kT \ln\langle\exp(-V/kT)\rangle_g$$

$$= \langle V \rangle_g - kT \ln\langle\exp(-\delta V/kT)\rangle_g \qquad (1)$$

where V is the solvent contribution to the excitation energy, δV is the deviation of V from its mean, and the subscript g indicates an average over the ground state ensemble. The second equality decomposes the perturbation free energy into a static term, $\Delta F_{st} = \langle V \rangle_g$, and a relaxation term, $\Delta F_{rlx} = -kT \ln\langle\exp(-\delta V/kT)\rangle_g$. The latter represents the dielectric relaxation of the solvent in response to the excited state charge redistribution.[48−50] It can always be expanded in powers of δV. The lowest term gives the dielectric relaxation free energy in the limit of a small perturbation (small δV), *i.e.*, in the linear response limit:

$$\Delta F_{rlx} = -\frac{1}{2kT}\langle\delta V^2\rangle_g + O(\delta V^3) \qquad (2)$$

If δV follows a Gaussian distribution, the higher order terms $O(\delta V^3)$ are exactly zero,[51] and the solvent response is always linear, regardless of the magnitude of the perturbation δV. Notice that it is the magnitude of the fluctuations of V that limits the applicability of the free energy expansion and not the magnitude of V itself.

If the rms fluctuations of V are much larger than kT, the exponential formula becomes essentially useless. Insufficient sampling of the negative tail of the probability distribution $p(\delta V)$ leads to systematic error, which can easily be mistaken for dielectric saturation, due to its sign.[50] A multiwindow or umbrella sampling strategy can then be used. Alternatively, the linear response approximation (2) may apply. Bulk water is sufficiently polarizable that this approximation appears to give reasonable results for fairly large perturbations, well beyond the limit $\langle\delta V^2\rangle_g^{1/2} \sim kT \sim \Delta F_{rlx}$.

2.4. Calculations with a Macroscopic Continuum Model. The contribution of solvent relaxation to the excitation free energy of (classical) tryptophan was also calculated using a macroscopic continuum model.[52] Tryptophan is viewed as a cavity in a solvent continuum, with each atom bearing a partial charge equal to its charge shift upon excitation. The free energy for this system, obtained by solving the Poisson−Boltzmann equation, is equal to the solvent contribution to the dielectric relaxation free energy, in response to tryptophan excitation.[50] The Poisson−Boltzmann calculations were done with the program Delphi.[53] 3-21G charges and Amber atomic radii were used; the solute dielectric constant was set to 1, and the ionic strength to 0. Calculations were done with χ_1 in the *trans*, *gauche*[+], and *gauche*[−] conformations (conformations minimized in vacuum with no electrostatic interactions).

3. Results

3.1. Comparison of Structural Properties from the Quantum and Classical Runs. *Solute and Solvent Intramolecular Degrees of Freedom.* The number of beads in our model is too small to give high accuracy for the quantum bond fluctuations, and the fluctuations of bond angles involving hydrogens (see ref 54, Discussion). For this, at least 20 beads would be needed. Thus, our results for the hardest degrees of freedom must be viewed as qualitative.

Both bond lengths and bond angles show appreciable quantum effects even at room temperature. For example, although the water bond angle has an average value of 107° in all three simulations, its rms fluctuation is larger by a factor of ∼2 in the quantum than in the classical runs; the values are 3° (classical), 6° (quantum, 5-bead), and 7° (quantum, 10-bead). The fluctuations of bond lengths also increase by a factor of ∼2 in the quantum runs. For example, the rms fluctuations of the water O−H bonds are 0.02, 0.04, and 0.04 Å for the classical, 5-bead, and 10-bead runs, respectively. The average O−H bond length is 1.009 Å in all three runs. The rms fluctuation of the O−H bond length in an isolated water molecule can be estimated from a quantum harmonic oscillator model[55] to be 0.1 Å. Thus the 5- and 10-bead estimates of 0.04 Å are too small. In theory, the limited number of beads in our model is expected to underestimate the O−H fluctuations. However, Kono *et al.*[54] showed that the probability distribution of a harmonic oscillator of this stiffness is fairly well fit by a 10-bead model at room temperature. Thus, the underestimate is probably mainly due to the parametrization of the force field;[38] *i.e.* the classical effective force constant is too stiff. However,
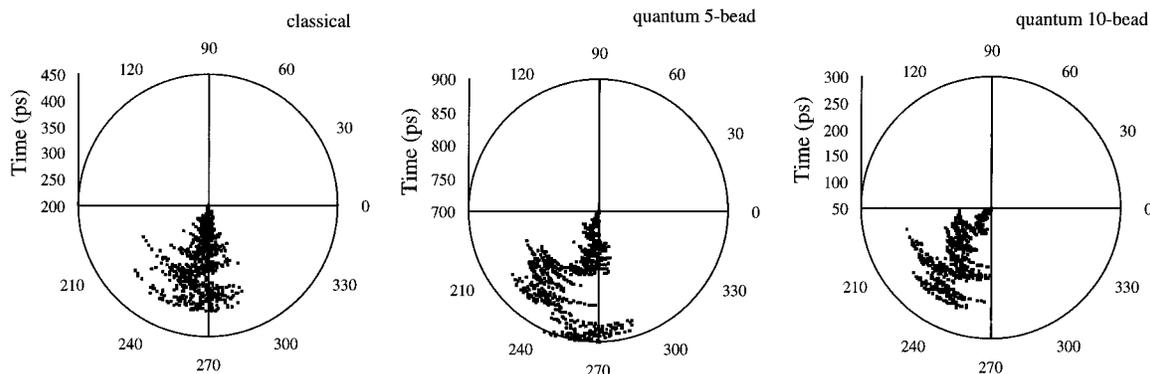
Figure 1. Tryptophan dihedral angle χ_2 as a function of time shown as dial plots: (a) classical; (b) 5-bead; (c) 10-bead.
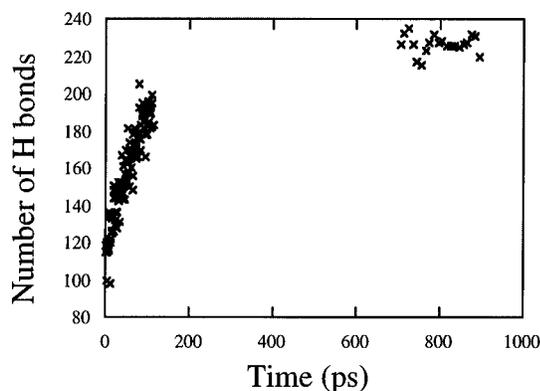
Figure 2. Total number of water−water hydrogen bonds of the 5-bead quantum system as a function of time, during the early equilibration phase, and the final data collection phase, of the simulation.

Figure 3. Oxygen−oxygen radial distribution functions from the classical, 5-bead and 10-bead simulations.

the relative magnitude of the quantum effects should be fairly insensitive to this force constant.

Bond lengths involving solute hydrogens behave similarly. For example, the rms fluctuations of the N−H bond lengths of the amino group are approximately twice as large in the quantum runs as in the classical: 0.03, 0.05, and 0.06 Å for the classical, 5-bead, and 10-bead runs. The average N−H bond length is 1.01 Å in all three cases. The quantum effects on the bond lengths involving two heavy atoms are somewhat smaller. For example, the rms fluctuations of the CA−CB bond lengths are 0.03, 0.04, and 0.05 Å for the classical, 5-bead, and 10-bead runs. The average CA−CB bond lengths are 1.54, 1.54, and 1.55 Å, respectively.

In contrast to these hard degrees of freedom, the quantum effects on the soft dihedral degrees of freedom are negligible at room temperature. For example, the average χ_1 angles are 50°, 52°, and 49° for the classical, 5-bead, and 10-bead runs. The corresponding rms fluctuations are 9°, 8°, and 8°, respectively. The differences between the three runs are within sampling errors. The fluctuations of the χ_2 angles (Figure 1) are somewhat larger than the χ_1 angles, and it is harder to reliably estimate them from the 200 ps 10-bead simulations carried out in this work. However, the classical and quantum fluctuations appear to agree within statistical error.

Water Hydrogen Bonds and Structure. The number of water hydrogen bonds is one of the first quantities we monitor for the equilibration of the dynamics runs. A hydrogen bond is assumed to be formed when the distance between a hydrogen and its hydrogen bond acceptor is ≤ 2 Å and the O−H−O angle is $> 135°$. Figure 2 shows the number of water hydrogen bonds as a function of time for the beginning of the equilibration process, which is carried out by Verlet dynamics with a weak coupling to a temperature bath. The number of hydrogen bonds is quite low, ∼100, after 30 ps. It then gradually increases to
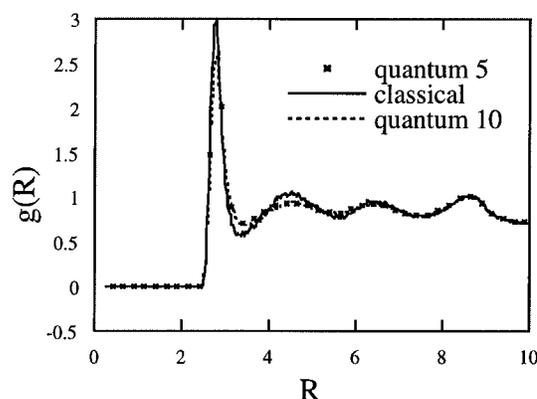
∼190 after 100 ps of Verlet dynamics. After several hundred more picoseconds of equilibration with Verlet followed by Langevin dynamics, the number of hydrogen bonds averaged over the last 200 ps is 260 ± 10. This can be compared with 227 ± 2 for the 5-bead run and 218 ± 2 for the 10-bead run. The results obtained from the 5-bead and 10-bead runs are quite similar, suggesting that the 5-bead representation has already accounted for most of the quantum effects on hydrogen bonding quite well at the temperature where the system is simulated. Quantum effects decrease the number of water hydrogen bonds formed.

The water O−O radial distribution functions for the three runs are shown in Figure 3. The results from the two quantum runs are quite close and differ from the classical runs. The results are qualitatively similar to those obtained by Rossky *et al.* on pure water,[6,7] except that we observe an exaggerated water structure, with two extra peaks, corresponding to the third and fourth hydration shells. Some overstructuring of this water model was also observed by Teleman *et al.*,[38] compared to rigid SPC water. (A slightly different flexible SPC model[56] gave a structure very similar to rigid SPC, however.[57]) Cutoff artifacts can be seen at the cutoff separation and presumably also contribute to the overstructuring. The presence of tryptophan, with its charged and hydrophobic groups, probably also contributes to the structuring. However, our results are similar to those of Rossky *et al.* in that the quantum effects *reduce* the degree of water structure. This is consistent with the reduced number of hydrogen bonds in the quantum runs.

3.2. Solvation and Excitation Energies. *Classical Simulation.* The solvent effect on the tryptophan absorption and emission properties is determined by the solvent contribution to the tryptophan excitation energies. These are dictated by the charge redistribution upon excitation and by the solvent electrostatic potential on the tryptophan atoms. In the classical

Simulations of Tryptophan in Solution

J. Phys. Chem. A, Vol. 101, No. 10, 1997 **1939**

TABLE 2: Ground and Excited State Dipole Moments

molecule	method	state	$|\mu|$ (D)	$|\delta\mu|^a$ (D)
tryptophan	3-21G	ground	13.93^b	
tryptophan	3-21G	1La	13.11^b	2.30
tryptophan	3-21G	1Lb	13.16^b	1.41
tryptophan	CNDO/S	ground	14.90^c	
tryptophan	CNDO/S	1La	13.00^c	5.96
tryptophan	CNDO/S	1Lb	14.39^c	1.53
indole	experiment	ground	2.13^d	
indole	experiment	1La	5.4^e	
indole	experiment	1Lb	$2.3-3.4^{d,e}$	
methylindole	CNDO/S	ground	1.15^c	
methylindole	CNDO/S	1La	6.48^c	5.60
methylindole	CNDO/S	1Lb	2.66^c	1.72
methylindole	ref 32^f	1La	6.9	6.0^b
methylindole	ref 58^g	1La	5.4	2.7^b
methylindole	ref 58	1Lb	2.1^g	0.4^b

^{a} Dipole shift between ground and excited state. ^{b} Calculated from atomic point charges. ^{c} Values from wave function and from atomic point charges are within 1% of each other. ^{d} Reference 75. ^{e} Reference 59. ^{f} Muino Callis charges.[32] ^{g} Charges from Westbrook et al.[58]
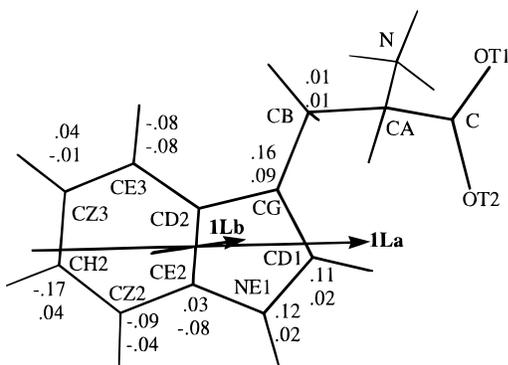
Figure 4. Tryptophan molecule, with arrows showing the dipole moment shifts associated with excitation (labeled 1La and 1Lb, respectively), from the CNDO/S calculation. The calculated dipole shifts are almost entirely contained in the plane of the figure. Atoms are labeled with the atomic partial charge shifts associated with excitation (upper numbers: 1La shifts; lower numbers: 1Lb shifts). When no numbers are given, atoms have negligible charge shifts.

simulation, the electrostatic potential ranges from -18 e Å^{-1} on the amino hydrogens to >100 e Å^{-1} on the carboxyl oxygens. The total tryptophan solvation energy of -160.5 kcal/mol is dominated by the carboxyl group (-106.3 kcal/mol), with -18.7 kcal/mol from the amino group, -35.1 kcal/mol from the indole group, and just -0.3 kcal/mol from the α and β carbon groups.

Charge redistribution in the ground and excited states is significant. In what follows, we report results based on semiempirical CNDO/S calculations and ab initio calculations at the 3-21G level. The ab initio charge shifts give generally poorer agreement with experimental results for indoles. However, it is of interest to compare the magnitude of quantum effects estimated with the two charge sets, to test the sensitivity of the calculation to the exact partial charge model. The charges and dipole moments are given in Tables 1 and 2; the charge and dipole shifts are also shown in Figure 4. The CNDO/S dipole moment shifts for tryptophan are 6.0 D (ground → 1La) and 1.5 D (ground → 1Lb). The results for methylindole are similar. The ground and excited state dipoles agree approximately with experimental values for indole (Table 2). Our ab initio dipole shifts for tryptophan are just 2.3 and 1.4 D, respectively. For comparison, the Muino and Callis INDO/S 1La result for methylindole is also 6.0 D,[32] while the INDO/S charges of Westbrook et al.[58] lead to smaller shifts of 2.7 and 0.4 D, respectively.

Experimentally, the solvent contribution to the average
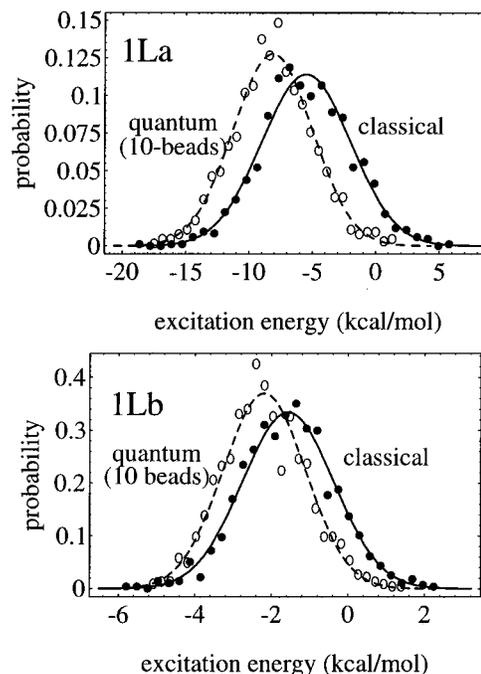
Figure 5. Probability distributions of the solvent contribution to the excitation free energies, using the CNDO/S charge shifts. The solid and dashed curves are Gaussian fits to the data.

excitation energy, $\langle V\rangle_g$, determines the solvent red shift of the absorption spectrum. In the 1La/CNDO excited state, the solvent contribution to the excitation energy is $\langle V\rangle_g = -5.5$ kcal/mol. Interactions with the indole group contribute -6.6 kcal/mol, with much smaller contributions from the amino, carboxyl, and aliphatic groups. This compares favorably with an experimental absorption red shift for 3-methylindole of -1500 cm$^{-1} = -4.3$ kcal/mol.[59] In the 1Lb/CNDO excited state, the average excitation energy due to solvent is -1.6 kcal/mol; interactions with the indole group contribute -2.1 kcal/mol, with much smaller contributions from the other groups. The experimental 1Lb red shift for 3-methylindole is -95 cm^{-1} $= -0.3$ kcal/mol.

In the 1La/3-21G and 1Lb/3-21G excited states, the carboxyl group makes a surprisingly large contribution of $+6$ kcal/mol to the solvation energy shift, with the indole group contributing just -1 kcal/mol. The average 1La/3-21G excitation energy due to solvent is $+5.0$ kcal/mol; the 1Lb/3-21G result is $+5.9$ kcal/mol. These results differ from the experimental methylindole shifts. It may well be that the ab initio excited state charges are not particularly good, as discussed above (Methods). However, because the experimental data are for indoles, which lack the charged carboxylate and amino groups of tryptophan, we cannot completely rule out a possible effect of the charged groups on the red shift. There are a number of cases in proteins where the presence of negatively charged groups around tryptophans appears to lead to blue-shifted spectra.

The 1La and 1Lb excitation energies fluctuate as a result of solute and solvent motions, and this is reflected experimentally in the broadening of the absorption and emission spectra. The probability distributions of the solvent contribution to the excitation energies are shown in Figure 5, from both the classical and the quantum simulations, using the CNDO/S charges. The distributions are approximately Gaussian in the thermally accessible range, as are the electrostatic potentials on the individual tryptophan atoms (not shown). The 3-21G charges also lead to similar shapes (not shown). The standard deviations of the distributions from the classical simulation, using the CNDO/S charges, are 3.5 kcal/mol (1La/CNDO) and 1.2 kcal/

TABLE 3: Solvent Contribution to Excitation Free Energies[a]

charges	state	method	$\langle V \rangle^b$	ΔF^c	$-(1/2kT)\langle \delta V^2 \rangle^d$	ΔF_{rlx}^e
CNDO/S	1La	classical	−5.51 (121)	−14.6	−10.4	not available[f]
CNDO/S	1La	5 bead	−6.55 (121)	−13.1	−8.4	not available
CNDO/S	1La	10 bead	−8.16 (67)	−14.0	−8.3	not available
CNDO/S	1Lb	classical	−1.57 (30)	−2.8 (4)	−1.21 (20)	−1.27
CNDO/S	1Lb	5 bead	−1.74 (33)	−2.6 (4)	−0.86 (14)	−0.85
CNDO/S	1Lb	10 bead	−2.19 (33)	−3.0 (4)	−0.99 (12)	−0.85
3-21G	1La	classical	5.02 (24)	3.5 (3)	−1.17 (26)	−1.51
3-21G	1La	5 bead	4.53 (69)	3.3 (8)	−1.25 (33)	−1.26
3-21G	1La	10 bead	3.83 (18)	2.8 (2)	−1.01 (15)	−1.07
3-21G	1Lb	classical	5.91 (13)	5.4 (1)	−0.48 (07)	−0.50
3-21G	1Lb	5 bead	5.54 (57)	4.8 (6)	−0.70 (17)	−0.73
3-21G	1Lb	10 bead	5.27 (07)	4.8 (1)	−0.42 (04)	−0.46

[a] Results in kcal/mol. Statistical error in last digits in parentheses. [b] Identical to the static component ΔF_{st} of excitation free energy. [c] Total excitation free energy $\Delta F_{st} + \Delta F_{rlx}$. [d] Linear response estimate of relaxation free energy ΔF_{rlx}. [e] Relaxation free energy from exponential formula. [f] Exponential formula not applicable due to limited conformational sampling.

mol (1Lb/CNDO). With the 3-21G charges, the widths are smaller (1.2 and 0.8 kcal/mol, respectively). The experimental 1La width for indole in glycerol (which includes both solvent and solute contributions) has been estimated to be 1040 cm^{-1}, or 2.9 kcal/mol, close to our CNDO/S result.

Quantum Simulations. The tryptophan solvation energies decrease somewhat going from 1 to 10 beads; the results (in kcal/mol) are −160.5 (2.0) (classical), −161.4 (2.5) (5 beads), and −163.0 (1.5) (10 beads) (standard errors in parentheses). Thus the ground state is more strongly solvated in the quantum simulations. Although the decrease is at the limit of the statistical error, it appears systematic and arises largely from the hydrogen atoms. The group solvation energies from the three simulations are all within statistical error, except for the amino group, and the 5-atom cycle in the indole ring, whose solvation energies decrease by about 1 and 2 kcal/mol, respectively.

The 1La and 1Lb excitation energies also decrease in the quantum simulations; for example, the 1La/CNDO results (kcal/mol) are −5.51 (1.21) (classical), −6.55 (1.21) (5 beads), and −8.16 (0.67) (10 beads). The 1Lb/CNDO results show the same trend; the results are −1.57 (0.30) (classical), −1.74 (0.30) (5 beads), and −2.19 (0.33) (10 beads). The classical → 10-bead energy decrease is larger than the estimated uncertainty. Thus, in the quantum simulations, the ground and excited states are both solvated more strongly than in the classical simulation, but the effect is stronger in the excited states than in the ground state. The 3-21G excitation energies also show the same systematic trend (Table 3).

The quantum probability distributions of the 1La and 1Lb excitation energies are shown in Figure 5. They are systematically about 10% narrower than the classical ones. Thus the 1La/CNDO widths are 3.5 kcal/mol (classical) and 3.2 kcal/mol (10 bead). The 1Lb/CNDO widths are 1.2 kcal/mol (classical) and 1.1 kcal/mol (quantum). The 3-21G trends are the same. In what follows, this quantum narrowing will translate directly into a systematically smaller dielectric response of the solvent, and is consistent with the weakening of the quantum water structure already discussed.

3.3. Relaxation Free Energies. *Classical Simulation.* The relaxation free energies are determined by the shape of the probability distribution of the excitation energies (eq 1). For both the 1La and 1Lb states, the probability distribution is approximately Gaussian (Figure 5). Except for the 1La/CNDO case, the modest fluctuations ($\langle \delta V^2 \rangle^{1/2} \sim kT$), and the approximately Gaussian shape, imply that the dielectric response of the solvent will follow linear response to a good approximation.[50,51] Furthermore, since $\langle \delta V^2 \rangle^{1/2} \sim kT$, the exponential formula should be fairly accurate and can therefore be used to

estimate deviations from the linear response. On the other hand, the 1La/CNDO excitation energy has fluctuations much larger than kT, so that the exponential formula is effectively useless. However, the linear response approximation is still expected to be accurate, based on studies of test charges and dipoles in water and other solvents.[60,61]

As an illustration of the convergence of the calculation, and the linearity of the solvent response, we first consider excitation to the 1La/3-21G state. For this state, the static part of the excitation free energy (eq 1) is $\Delta F_{st} = \langle V \rangle_g = 5.02$ kcal/mol. The total excitation free energy, from the exponential formula, is $\Delta F = 3.51$ kcal/mol. Therefore, the relaxation free energy in response to the excitation is $\Delta F_{rlx} = -1.51$ kcal/mol. The second-order estimate of the relaxation free energy is $-(1/2kT)\langle \delta V^2 \rangle_g = -1.17$ kcal/mol. The third- and fourth-order free energy terms are estimated together to be −0.12 kcal/mol. Systematic error in the free energy associated with insufficient sampling of the tails of the probability distribution $p(\delta V)$ is estimated to be small (<0.1 kcal/mol). Systematic error associated with inadequate sampling of conformational sub-states[62] is expected to be small, since our simulations are restricted to just one of the major conformations of tryptophan (g^+, *perp*). Thus the uncertainty should be dominated by random statistical error, estimated to be just 0.2 kcal/mol for the first- and second-order free energy terms, and 0.3 kcal/mol for the total free energy. These results are consistent with the presence of little or not dielectric saturation, as expected for such a moderate perturbation.[60]

With the CNDO/S charges, the 1La free energies (kcal/mol) are much larger in magnitude, so that the perturbation method is less reliable, and the error bars notoriously difficult to estimate. Indeed, we must rely on the linear response approximation, for which an a priori error estimate is difficult. We obtain a large relaxation: $\Delta F_{rlx} = -(1/2kT)\langle \delta V^2 \rangle_g = -10.4$ kcal/mol. For 1Lb/CNDO, $\Delta F_{rlx} = -1.3$ kcal/mol, with negligible dielectric saturation.

To compare the relaxation free energies to experimental Stokes shifts, we need to invoke the relation between dielectric relaxation energies and free energies, discussed below, and in the Appendix. For the moment, we simply note that the relaxation free energy, following 1La excitation of methylindole in water, can be estimated to be −5.45 kcal/mol, in better agreement with the CNDO/S result than the 3-21G result (Table 3).

Quantum Simulations. The quantum relaxation free energies differ in a systematic way from the classical results, as did the quantum excitation energies seen above (Table 3). For the 1La/CNDO state, the relaxation free energies (in kcal/mol) are −10.4 (classical), −8.4 (5 bead), and −8.3 (10 bead). Dielectric

Simulations of Tryptophan in Solution

J. Phys. Chem. A, Vol. 101, No. 10, 1997 **1941**

relaxation is weaker in the quantum case, consistent with the weaker quantum water structure seen above. For the 1Lb/CNDO state, the relaxation free energies are −1.21 (20) (classical), −0.86 (20) (5 bead), and −0.99 (12) (10 bead) (standard errors on the last digits in parentheses).

With the 3-21G charges, the 1La relaxation free energies are smaller (Table 3), but again, relaxation is weaker in the quantum case. The same trend is seen using the Muino and Callis charge shifts,[32] as well as the Westbrook *et al.* charge shifts[58] (not shown).

The classical → 10-bead relaxation free energy decreases are about equal to the standard error. However, considering the consistent trend for both excited states and four different charge models, along with the systematic variation of the hydrogen solvation energies (above), and the systematic decrease in water structure, this relaxation decrease appears to be a real effect of the quantization.

3.4. Relaxation Free Energies from a Continuum Model. In addition to the molecular dynamics calculations described above, we have calculated the contribution of solvent relaxation to the excitation free energies from a continuum model, both as a consistency check and to aid in the interpretation of the microscopic simulations. Indeed, disagreement would suggest that local details of the molecular interactions are important.

The complete tryptophan excitation free energies cannot be calculated from the continuum model alone; an estimate of the vacuum excitation free energy would also be needed. In order to compare the continuum model directly to the molecular dynamics results, we focus instead on the dielectric relaxation free energy ΔF_{rlx} in response to the excitation. In the continuum model, the solvent contribution to ΔF_{rlx} is obtained from a Poisson−Boltzmann calculation that includes only the atomic partial charge shifts associated with the excitation. The electrostatic free energy to solvate the charge shifts is identical to the dielectric relaxation free energy.[50]

Calculations were done with χ_1 in the *trans*, *gauche*$^+$, and *gauche*$^-$ conformations. Our molecular dynamics simulations were all done in the *gauche*$^+$ state. The 3-21G charge shifts were used.

The solvent relaxation free energy for 1La excitation varies between −0.5 and −0.6 kcal/mol, depending on the conformation and the exact Poisson−Boltzmann protocol. The solvent relaxation free energy for 1Lb excitation is −0.2 kcal/mol. For comparison, the Onsager free energy of the corresponding dipole in a spherical cavity is −1.4 (1La) and −0.4 kcal/mol (1Lb), assuming a tryptophan radius of 3.2 Å. The molecular dynamics results were −1.2 kcal/mol for 1La/3-21G and −0.5 kcal/mol for 1Lb/3-21G. While the Poisson−Boltzmann results are smaller, the approximate magnitude and the trend of a smaller relaxation for 1Lb agree with the molecular dynamics results.

3.5. Time-Dependent Solvent Relaxation. Immediately after excitation, the solvent is in equilibrium with the ground state charge distribution, and the solvent contribution $V(0)$ to the nonequilibrium excitation energy is large. As the solvent gradually adjusts to the excited state charge distribution, the solvent contribution $V(t)$ to the nonequilibrium energy decreases and finally reaches its equilibrium excited state value V_e. As the energy relaxation occurs, the red shift of the fluorescence spectrum due to solvation increases.[63] The time-dependent red shift is characterized experimentally through the Stokes shift response function:[64]

$$S(t) = \frac{V(t) - V_e}{V(0) - V_e} \tag{3}$$
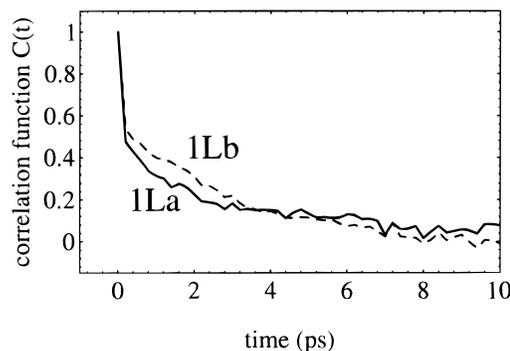
Figure 6. Normalized correlation function $C(t)$ (eq 4) of the 1La (solid) and 1Lb (dashed) excitation energies (based on the CNDO/S charge shifts).

Linear response theory predicts that this function is equal to the equilibrium correlation function $C(t)$ of the excitation energy in the unperturbed, ground, state[65,66]

$$C(t) = \frac{\langle \delta V(0)\, \delta V(t) \rangle_g}{\langle \delta V^2 \rangle_g} \tag{4}$$

where the brackets represent an average over the ground state ensemble, and δV represents the deviation of the excitation energy from its mean. In the case of indole and 3-methylindole in water, the time dependence of the fluorescence red shift is believed to be dominated by dielectric relaxation of the solvent.[31] We can calculate the solvent contribution to δV and the corresponding correlation function $C(t)$ function from our classical simulations. (The calculation of quantum time-dependent correlation functions[17,67] is beyond the scope of this work.)

The normalized correlation function $\langle \delta V(0)\, \delta V(t) \rangle_g / \langle \delta V^2 \rangle_g$ is plotted in Figure 6 for the excited states 1La/CNDO and 1Lb/CNDO. The 3-21G charges lead to very similar results (not shown). The uncertainty in the correlation functions is estimated, from the apparent relaxation times of 1−2 ps and the total simulation length of 200 ps, to be about ±15%.[68] Over half of the relaxation occurs in the first 200 fs, and most of the remaining relaxation occurs within the next few picoseconds. The short-time portion of the curve (below 0.2 ps) cannot be resolved further, because trajectory frames were only stored every 0.2 ps. Experimental data for tryptophan is not available on the femtosecond time scale. However, recent ultrafast spectroscopic measurements have demonstrated a large femtosecond solvent response for other solutes in water,[64] and molecular dynamics simulations of 3-methylindole in water also suggest femtosecond solvent relaxation.[31]

4. Discussion

4.1. Convergence and Limitations of the Simulations. An obvious limitation of our quantum simulations is the modest number of beads used. A theoretical analysis of the path integral representation of the harmonic oscillator[54] shows for example that for an oscillator of frequency 1000 cm^{-1}, a 5-bead model reproduces the room temperature energy and free energy within 10% and 4%, respectively, while a 10-bead model reproduces them within 4% and 1%, respectively. The probability distribution of the oscillator stretch is reproduced accurately with just 5 beads. On the other hand, for a 3000 cm^{-1} oscillator at room temperature, the 10-bead model has 15% and 5% errors for the energy and free energy, respectively, while the 5-bead model is even further off. Thus, our 10-bead representation should be accurate for the low and moderate frequency modes; for bond

stretching modes, and the bending modes involving hydrogens, it should still be qualitatively reasonable although 20 beads or more would no doubt be needed to achieve high accuracy.[16] The apparent convergence for the structural and energetic properties examined above, going from 5 to 10 beads, suggests that the 10-bead model is reasonably accurate for many purposes.

Sampling is another problem in path integral simulations, due to the coexistence of stiff quantum springs with soft collective degrees of freedom.[69] This problem may worsen as the number of beads increases. Velocity reassignment schemes, or Langevin dynamics algorithms, have been suggested to alleviate this,[5,15] and indeed, we see marked improvement in sampling going from the simple Verlet algorithm to Langevin dynamics (not shown). Overall, based on the small apparent error bars for the properties examined, the approximate agreement between the Verlet and Langevin dynamics, and the systematic nature of the quantum effects observed, it appears that with 5−10 beads, and 250−400 ps of Langevin dynamics, we have achieved reasonable sampling.

The choice of force field and treatment of long-range interactions is another difficulty. Existing force fields have been parametrized without exception for classical simulations, and furthermore, the flexible water model used here has not been extensively parametrized and tested.[38] A polarizable water model might have been better suited to describe the interactions with the tryptophan zwitterion. The truncation of electrostatic forces used here also introduces some artifacts,[39−41] although the solute studied is neutral. In particular, overstructuring of the water may lead to an overestimate of the dielectric relaxation. Finally, accurate calculations of the excited state charges of tryptophan are difficult, and different methods lead to different energetics. Nevertheless, these approximations should affect the classical and quantum simulations to about the same degree, so that we can still analyze the magnitude of quantum effects with reasonable confidence.

4.2. Quantum Effects on Structure and Energetics.
Consistent with previous studies, we see that even at room temperature, quantum effects are significant for structure, fluctuations, and energetics. The effect is especially noticeable on the water structure, with the average number of hydrogen bonds decreasing from 260 in the classical simulation to 218 in the 10-bead simulation. Kuharski and Rossky[6] pointed out that the decrease in water structure mimics (crudely) an increase in temperature by about 50 degrees. The increased fluctuations of the hard degrees of freedom in the water and the tryptophan are similar to previous results for proteins,[22] while the soft tryptophan χ_1 and χ_2 dihedrals are not affected by the quantization, to within statistical errors. Thus the quantization is not expected to directly affect the soft degrees of freedom in a protein molecule. Nevertheless, the energetic effects seen here imply that quantization could have an indirect effect on protein dihedrals, by modifying the relative stabilities of different dihedral wells. For example, in the present study, the quantization decreases the solvation energy of the amino group by 1.1 kcal/mol and increases that of the carboxyl group by 1.5 kcal/mol; in a protein environment, this type of effect would favor arrangements of the protein where the amino is more exposed and the carboxyl less so.

The energetic effects of increasing the bead number in our simulations are small but systematic, suggesting that they are real effects of quantization. The effect on the solvation energy and free energy is quite significant (Table 3). Quantization decreases both the ground and excited state solvation energies by 1−2 kcal/mol. The solvent dielectric relaxation in response
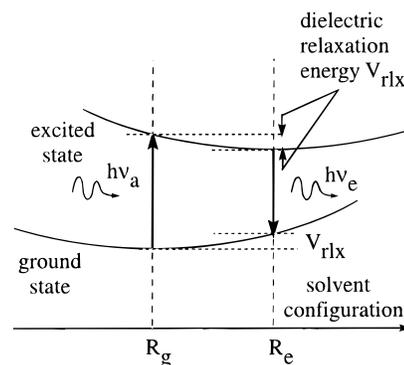
Figure 7. Schematic view of ground and excited state energy surfaces. The horizontal axis represents a collective solvent coordinate along which relaxation occurs. The dielectric relaxation energy following excitation, corresponds to a solvent rearrangement from R_g to R_e, and to a relaxation energy V_{rlx}. Relaxation following emission releases the same relaxation energy V_{rlx} (we assume equal curvatures of the ground and excited state surfaces).

to excitation, which gives rise experimentally to the fluorescence Stokes shift, is systematically about 20% smaller in the quantum case. This effect also mimics a temperature increase, as did the water structure decrease. Convergence with respect to the number of beads may be incomplete, so that with more beads, dielectric relaxation would decrease further.

4.3. Relation between Relaxation Free Energies and Experimental Stokes Shifts.
The connection between the solvation free energy and the experimental Stokes shift is straightforward but has occasionally been neglected in the recent literature. For example, Stokes shifts have sometimes been incorrectly compared to the excitation free energy;[30] in fact, they are directly related to the relaxation energy in response to excitation. Indeed, if $\Delta\nu_a$ and $\Delta\nu_e$ are the absorption and emission shifts of the chromophore in solution relative to vacuum, the Stokes shift $h\Delta\nu_a - h\Delta\nu_e$ measures the dielectric relaxation of the environment[33,34] in response to the charge redistribution upon absorption and emission (Figure 7). Assuming the curvatures of the energy surfaces around the ground and excited states are the same, the dielectric relaxation in response to the initial excitation, and that in response to the subsequent emission, are equivalent. This is likely to be a good approximation, as shown by detailed simulation studies of charged solutes in acetonitrile, a solvent somewhat less polar than water.[61] Therefore, the Stokes shift will be twice the relaxation energy in response to excitation. This relaxation energy, in turn, is simply related to the relaxation free energy. Indeed, it is known for a wide class of systems, including continuum models, that the relaxation free energy is just half the relaxation energy.[28,33,34] Therefore, the Stokes shift is just 4 times the relaxation free energy:

$$h\Delta\nu_a - h\Delta\nu_e = 4F_{rlx} \qquad (5)$$

We have calculated only the direct solvent contribution to the relaxation free energy. Assuming intramolecular relaxation to be small, or at least independent of solvent relaxation, we can directly compare our results to the experimental Stokes shift, typically measured by comparing fluorescence spectra in water and in a glassy environment. We should note, however, that it may be problematic to consider the solvent relaxation separately from the intramolecular relaxation. Indeed, in simulation studies of charged perturbations in the protein cytochrome c, a very large coupling was observed between dielectric relaxation by the protein and solvent.[50]

With this caveat, we can compare our results to experimental data for indole and methylindole in various solvents. The

Simulations of Tryptophan in Solution

J. Phys. Chem. A, Vol. 101, No. 10, 1997 **1943**

estimated emission shift for 3-methylindole in water is 3800 cm^{-1}, or 10.9 kcal/mol.[32] This is half the Stokes shift, since absorption is not considered. It corresponds to a relaxation free energy of 5.45 kcal/mol. The Stokes shift of indole relative to hexane is 4.6 kcal/mol in acetonitrile and 9.1 in butanol.[30,70] The Stokes shift of methylindole relative to cyclohexane is 8.5 kcal/mol in acetonitrile and 9.1 kcal/mol in butanol.[71] These shifts correspond to relaxation free energies between 2.28 and 1.15 kcal/mol.

Our calculated relaxation free energies range depend on the charge model used (Table 3). The 1La/CNDO results (8.3−10.4 kcal/mol) are larger than the methylindole experimental estimate in water (5.45 kcal/mol), but of the same order of magnitude. The INDO/S charge shifts of Muino and Callis[32] give very similar results. The 3-21G results are considerably smaller. This probably reflects a poor description of the excited state (although our data do not allow us to completely rule out a real decrease in the excited state solvation, going from methylindole to tryptophan, associated with the charged carboxyl and amino groups).

5. Conclusions

We have used classical and quantum molecular dynamics simulations of tryptophan in water to probe quantum effects on a biologically relevant molecule, with both hard (bond, angle), and soft dihedral degrees of freedom, of the kind that determine the fold of proteins and peptides. The path integral simulations were implemented in command scripts for the program X-PLOR,[45] using only standard features of the program. Scripts are available from the authors on request. The simulations have some obvious limitations, especially truncation of electrostatic interactions, lack of any reparametrization of the force field, and a limited number of beads in the quantum representation. Nevertheless, a number of qualitative results are of interest. Quantum effects on structure, fluctuations, and energetics are significant, even at room temperature, as noted for other systems by previous authors. Although the soft dihedral degrees of freedom are not directly affected by the quantization, they may be affected indirectly, by changes in the solvation of alternate conformations. While the method used did not allow us to study the actual dynamics of the system, the increased range of fluctuations available, and the decrease in water structure, will have a significant effect on the local and collective motions of a large solute such as a protein. With the path integral methodology readily available in simulation packages, it will become necessary to specifically parametrize force fields, as more detailed quantum studies become routine.

The solvent relaxation in response to tryptophan photoexcitation was also studied, using a simple, atomic point charge description of the ground and excited states. We have not attempted to obtain highly accurate excited state charges, nor to do fully quantitative calculations of tryptophan's spectroscopic properties. This would require more sophisticated tools, such as hybrid classical/quantum simulations[32] that take into account the indole polarizability, possibly a polarizable water model, and multiwindow, free energy perturbation calculations. Our truncation of long-range electrostatic interactions also introduces artifacts, seen for example in the radial distribution functions. Nevertheless, we obtain approximate agreement with experiment for a number of properties, and furthermore, quantum effects should be fairly robust with respect to the exact charge shifts and the use of a long-range cutoff. The distribution of excitation energies is found to be nearly Gaussian in the thermal accessible range, indicating a nearly linear dielectric response of the solvent, as noted by Levy et al.[30] for methylindole excitation.

Quantum effects reduce the dielectric relaxation in all cases, consistent with the weakening of solvent structure in the quantum runs. Comparison is made to Stokes shifts in polar solvents, by observing that the relaxation free energy is just $^1/_4$ of the Stokes shift, an occasionally neglected relation. The calculated relaxation, using the CNDO/S charges, appears larger than experimental estimates for indole and 3-methylindole in various solvents. This may be due to coupling between intramolecular and solvent relaxation, found to be important in simulation studies of proteins;[50] or it may be due to overstructuring of the liquid induced by the electrostatic cutoff. However, the magnitude of the quantum correction to the Stokes shift is likely to be more robust than the absolute value and appears to be significant, representing up to 20−30% of the solvent relaxation free energy. It is not at all clear that effective classical potentials can accurately capture such large effects in all cases. Therefore, approaches such as those used here should prove useful for quantitative studies of dielectric relaxation in biological macromolecules, including processes such as electron transfer and photosynthesis.

Appendix: Relation between Dielectric Relaxation Energy and Free Energy

Because the relation between the relaxation energy and the relaxation free energy[28,33,34] has occasionally been neglected in the recent literature, we give a proof below.

Consider a molecular system such as a folded protein, or a tryptophan molecule, perturbed by a set of external charges. Let $\mathbf{f} = (\mathbf{f}_1, \mathbf{f}_2, ..., \mathbf{f}_n)$, where $\mathbf{f}_i$ is the perturbing field produced on atom i. If the perturbation is small, it contributes a linear term to the energy, of the form:

$$V = -\mathbf{x}\cdot\mathbf{f} \qquad (6)$$

where $\mathbf{x}$ represents the structural relaxation of the system. For simplicity, we can assume that $\mathbf{x}$ is also a $3n$ vector. However, the exact form of $\mathbf{x}$, and its physical nature, depend on the system. In some cases (e.g., for a macroscopic dielectric continuum), the dot product must be replaced by a volume or a surface integral. However, the linear form of V is retained, and the following arguments remain valid.

Let us define the instantaneous deviation $\boldsymbol{\delta}\mathbf{x}$ of $\mathbf{x}$ by

$$\mathbf{x} = \langle\mathbf{x}\rangle_0 + \boldsymbol{\delta}\mathbf{x} \qquad (7)$$

where $\langle\mathbf{x}\rangle_0$ is the ensemble average of $\mathbf{x}$ in the absence of the perturbing charges. Then

$$V = -\langle\mathbf{x}\rangle_0\cdot\mathbf{f} - \boldsymbol{\delta}\mathbf{x}\cdot\mathbf{f}$$

$$= V_{\text{stat}} + V_{\text{rlx}} \qquad (8)$$

We shall see that the second term, denoted V_{rlx}, is precisely the relaxation energy.

In the linear response regime, we have

$$\langle \boldsymbol{\delta x} \rangle_f = \boldsymbol{\alpha f} \tag{9}$$

where $\boldsymbol{\alpha}$ is the generalized susceptibility in response to $\mathbf{f}$,[72] which is a $3n \times 3n$ matrix in this case, but can be an integral operator in other cases (see below). The subscript f represents an ensemble average in the presence of the perturbation $\mathbf{f}$. Now assume that we introduce the perturbation gradually, scaling $\mathbf{f}$ by a coupling constant λ that varies gradually from 0 to 1. For a particular λ we have (with obvious notations)

$$V(\lambda) = -\lambda \langle \mathbf{x} \rangle_0 \cdot \mathbf{f} - \lambda \boldsymbol{\delta x} \cdot \mathbf{f}$$

$$\partial V / \partial \lambda = -\langle \mathbf{x} \rangle_0 \cdot \mathbf{f} - \boldsymbol{\delta x} \cdot \mathbf{f}$$

$$\frac{\partial F}{\partial \lambda}(\lambda) = \left\langle \frac{\partial V}{\partial \lambda} \right\rangle_\lambda = -\langle \mathbf{x} \rangle_0 \cdot \mathbf{f} - \langle \boldsymbol{\delta x} \rangle_\lambda \cdot \mathbf{f}$$

$$= -\langle \mathbf{x} \rangle_0 \cdot \mathbf{f} - \lambda \mathbf{f} \cdot \boldsymbol{\alpha f} \tag{10}$$

Notice that in the third equation, the first term on the right is a constant, unaffected by the ensemble averaging $\langle \ \rangle_\lambda$. Integrating the last equation from $\lambda = 0$ to $\lambda = 1$, we have finally

$$F = -\langle \mathbf{x} \rangle_0 \cdot \mathbf{f} - {}^1/_2 \mathbf{f} \cdot \boldsymbol{\alpha f} \tag{11}$$

The first term is the work to introduce the perturbing charges, while constraining the system so that it cannot adjust; *i.e.*, it retains its unperturbed probability distribution. The second term is then the relaxation free energy, with the usual quadratic form of linear response.

The first term is purely enthalpic, and comparing to (8), we can identify it with the static part of the perturbation energy, $\langle V_{\text{stat}} \rangle_f$. The remainder of the perturbation energy is then the relaxation energy. Taking the ensemble average of V_{rlx} and using (9), we then find the required relation

$$\langle V_{\text{rlx}} \rangle_f = -\mathbf{f} \cdot \boldsymbol{\alpha f}$$

$$= 2F_{\text{rlx}} \tag{12}$$

This formalism has been applied recently to several biological systems,[28,73,74] including (*i*) nondiffusive molecular systems (a folded protein in vacuum with atomic point partial charges); (*ii*) a set of fixed, polarizable, atomic, point charges (a model commonly used for proteins); and (*iii*) macroscopic continuum models. For diffusive systems, such as the tryptophan in water considered here, the perturbation energy and the susceptibility operator take on a more complicated form involving integral operators. It is not clear to us whether the simple relation between F_{rlx} and $\langle V_{\text{rlx}} \rangle$ will remain valid or not for this case, however, if we assume the solvent response is continuum-like, we expect that it will still hold at least approximately.

References and Notes

(1) Frauenfelder, H.; Wolynes, P. *Science* **1985**, *229*, 337.

(2) Chance, B. *Tunneling in Biological Systems*; Academic Press: New York, 1979.

(3) de Vault, D. *Quantum Mechanical Tunneling in Biological Systems*; Cambridge University Press: New York, 1979.

(4) Chandler, D. *Quantum Theory of Solvation*. *J. Phys. Chem.* **1984**, *88*, 3400−3407.

(5) Berne, B.; Thirumalai, D. *Annu. Rev. Phys. Chem.* **1986**, *37*, 401.

(6) Kuharski, R.; Rossky, P. A quantum mechanical study of structure in liquid H_2O and D_2O. *J. Chem. Phys.* **1985**, *82*, 5164−5177.

(7) Del Buono, G.; Rossky, P.; Schnitker, J. Model dependence of quantum isotope effects in liquid water. *J. Chem. Phys.* **1991**, *95*, 3728−3737.

(8) Thirumalai, D.; Hall, R.; Berne, B. A path integral Monte Carlo study of liquid neon and the quantum effective pair potential. *J. Chem. Phys.* **1984**, *81*, 2523−2527.

(9) Morales, J.; Nuevo, M. Path integral molecular dynamics methods: application to neon. *J. Comput. Chem.* **1995**, *16*, 105−112.

(10) Chakravarty, C. Melting of neon clusters: path integral Monte Carlo simulations. *J. Chem. Phys.* **1995**, *102*, 956.

(11) Böhm, M.; Ramirez, R. Dynamics of the carbon nuclei in C_{60} studied by Feynman path integral quantum Monte Carlo simulations. *J. Phys. Chem.* **1995**, *99*, 12401−12408.

(12) Zheng, C.; McCammon, J.; Wolynes, P. Quantum simulation of nuclear rearrangement in electron transfer reactions. *Proc. Natl. Acad. Sci. U.S.A.* **1989**, *86*, 6441−6444.

(13) Gai, H.; Garrett, B. Path integral calculations of the free energies of hydration of hydrogen isotopes (h, d, and mu). *J. Phys. Chem.* **1994**, *98*, 9642−9648.

(14) Gai, H.; Dang, L.; Schenter, G.; Garrett, B. Quantum simulation of aqueous ionic clusters. *J. Phys. Chem.* **1995**, *99*, 13303−13306.

(15) Pomes, R.; Roux, B. Quantum effects on the structure and energy of a protonated linear chain of hydrogen bonded water molecules. *Chem. Phys. Lett.* **1995**, *234*, 416−424.

(16) Straus, J.; Calhoun, A.; Voth, G. Calculation of solvent free energies for heterogeneous electron transfer at the water-metal interface: classical vs. quantum behavior. *J. Chem. Phys.* **1995**, *102*, 529−539.

(17) Cao, J.; Voth, G. The formulation of quantum statistical mechanics based on the Feynman path centroid density. III. Phase space formalism and analysis of centroid molecular dynamics. *J. Chem. Phys.* **1994**, *101*, 6157−6167.

(18) Calhoun, A.; Pavese, M.; Voth, G. Finite temperature quantum dynamics on the IBM SP2. Tech. Rep. 11, Cornell Theory Center, Summer 1996.

(19) Amara, P.; Hsu, D.; Straub, J. Global energy minimum searches using an approximate solution of the imaginary time Schrödinger equation. *J. Phys. Chem.* **1993**, *97*, 6715−6721.

(20) Kuriyan, J.; Osapay, K.; Burley, S.; Brünger, A.; Hendrickson, W.; Karplus, M. *Proteins* **1991**, *10*, 340.

(21) Burling, F.; Weis, W.; Flaherty, K.; Brünger, A. Direct observation of protein solvation and discrete disorder with experimental crystallographic phases. *Science* **1996**, *271*, 72−77.

(22) Zheng, C.; Wong, C.; McCammon, J.; Wolynes, P. Quantum simulation of ferrocytochrome c. *Nature* **1988**, *334*, 726−728.

(23) Wong, C.; Zheng, C.; Shen, J.; McCammon, J.; Wolynes, P. Cytochrome c: a molecular proving ground for computer simulations. *J. Phys. Chem.* **1993**, *97*, 3100−3110.

(24) Pierce, D.; Boxer, S. Dielectric relaxation in a protein matrix. *J. Phys. Chem.* **1992**, *96*, 5560−5566.

(25) Steffen, M.; Lao, K.; Boxer, S. Dielectric asymmetry in the photosynthetic reaction center. *Science* **1994**, *264*, 810−816.

(26) Warshel, A.; Russell, S. Calculations of electrostatic effects in biological systems and in solutions. *Q. Rev. Biophys.* **1984**, *17*, 283−342.

(27) Simonson, T.; Perahia, D.; Bricogne, G. Intramolecular dielectric screening in proteins. *J. Mol. Biol.* **1991**, *218*, 859−886.

(28) Simonson, T.; Perahia, D.; Brünger, A. T. Microscopic theory of the dielectric properties of proteins. *Biophys. J.* **1991**, *59*, 670−90.

(29) Gordon, H.; Jarrell, H.; Szabo, A.; Willis, K.; Somorjai, R. Molecular dynamics of the conformational dynamics of tryptophan. *J. Phys. Chem.* **1992**, *96*, 1915−1921.

(30) Levy, R.; Westbrook, J.; Kitchen, D.; Krogh-Jespersen, K. Solvent effects on the adiabatic free energy difference between the ground and excited states of methylindole in water. *J. Phys. Chem.* **1991**, *95*, 6756−6758.

(31) Muino, P.; Harris, D.; Berryhill, J.; Hudson, B.; Callis, P. Simulation of solvent dynamics effects on the fluorescence of 3-methyl indole in water. In *SPIE* **1992**, *1640*, 240.

(32) Muino, P.; Callis, P. Hybrid simulations of solvation effects on electronic spectra: indoles in water. *J. Chem. Phys.* **1994**, *100*, 4093−4109.

(33) Marcus, R. Electrostatic free energy and other properties of states having nonequilibrium polarization. *J. Chem. Phys.* **1956**, *24*, 979−989.

(34) Marcus, R. *Annu. Rev. Phys. Chem.* **1964**, *15*, 155.

(35) Smolyar, A.; Wong, C., manuscript in preparation (1997).

(36) Reimers, J. CNDO program. Tech rep., University of Sydney, 1985.

(37) Weiner, S.; Kollman, P.; Nguyen, D. T.; Case, D. An all atom force field for simulations of proteins and nucleic acids. *J. Comput Chem.* **1986**, *7*, 230−252.

(38) Teleman, O.; Jonsson, B.; Engstrom, S. A molecular dynamics simulation of a water model with intramolecular degrees of freedom. *Mol. Phys.* **1987**, *60*, 193−203.

(39) Brooks, C., III.; Brünger, A. T.; Karplus, M. Active site dynamics in proteins: a stochastic boundary molecular dynamics approach. *Biopolymers* **1985**, *24*, 843−865.

(40) Prévost, M.; van Belle, D.; Lippens, G.; Wodak, S. Computer simulations of liquid water: treatment of long-range interactions. *Mol. Phys.* **1990**, *71*, 587−603.

(41) Schreiber, H.; Steinhauser, O. Molecular dynamics studies of solvated polypeptides: why the cutoff scheme does not work. *Chem. Phys.* **1992**, *168*, 75−89.

(42) Berendsen, H.; Postma, J.; van Gunsteren, W.; DiNola, A.; Haak, J. Molecular dynamics with coupling to an external bath. *J. Chem. Phys.* **1984**, *811*, 3684−3690.

(43) Dezube, B.; Dobson, C.; Teague, C. Conformational analysis of tryptophan in solution using nuclear magnetic resonance methods. *J. Chem. Soc., Perkin Trans. 2* **1981**, 730−735.

(44) Janin, J.; Wodak, S.; Levitt, M.; Maigret, B. *J. Mol. Biol.* **1978**, *125*, 357−386.

(45) Brünger, A. T. X-PLOR *version 3.1, A System for X-ray crystallography and NMR*; Yale University Press: New Haven, CT, 1992.

(46) McQuarrie, D. *Statistical Mechanics*; Harper and Row: New York, 1975.

(47) Beveridge, D.; DiCapua, F. Free energy via molecular simulation: Applications to chemical and biomolecular systems. *Annu. Rev. Biophys. Biophys. Chem.* **1989**, *18*, 431−492.

(48) Chandler, D. The dielectric constant and related equilibrium properties of molecular fluids: interaction site cluster theory analysis. *J. Chem. Phys.* **1977**, *67*, 1113−1124.

(49) Stell, G.; Patey, G.; Hoye, J. Dielectric constants of fluid models: statistical mechanical theory and its quantitative implementation. *Adv. Chem. Phys.* **1981**, *48*, 183−328.

(50) Simonson, T.; Perahia, D. Microscopic dielectric properties of cytochrome c from molecular dynamics simulations in aqueous solution. *J. Am. Chem. Soc.* **1995**, *117*, 7987−8000.

(51) Levy, R.; Belhadj, M.; Kitchen, D. Gaussian fluctuation formula for electrostatic free energy changes. *J. Chem. Phys.* **1991**, *95*, 3627−3633.

(52) Sharp, K.; Honig, B. Electrostatic interactions in macromolecules: theory and applications. *Annu. Rev. Biophys. Biophys. Chem.* **1991**, *19*, 301−332.

(53) Sharp, K. DelPhi, Version 3.0. Columbia University, 1988.

(54) Kono, H.; Takasaka; Lin, S. Extraction of ground state properties by discretized path integral formulations. *J. Chem. Phys.* **1988**, *89*, 3233−3239.

(55) Landau, L.; Lifschitz, E. *Quantum Mechanics*; Pergamon Press: New York, 1980.

(56) Anderson, J.; Ullo, J.; Yip, S. Molecular dynamics simulation of dielectric properties of water. *J. Chem. Phys.* **1987**, *87*, 1726−1732.

(57) Watanabe, K.; Klein, M. Effective pair potentials and the properties of water. *Chem. Phys.* **1991**, *131*, 157−167.

(58) Westbrook, J.; Levy, R.; Krogh-Jespersen, K. Solvent effects on the adiabatic free energy difference between the ground and excited states of methylindole in water. *J. Comput. Chem.* **1992**, *13*, 979−989.

(59) Lami, H.; Glasser, N. *J. Chem. Phys.* **1986**, *84*, 597.

(60) Smith, P.; van Gunsteren, W. Predictions of free energy differences from a single simulation of the initial state. *J. Chem. Phys.* **1994**, *100*, 577−584.

(61) Maroncelli, M. Computer simulations of solvation dynamics in acetonitrile. *J. Chem. Phys.* **1991**, *94*, 2084−2103.

(62) Hodel, A.; Simonson, T.; Fox, R. O.; Brünger, A. T. Conformational substates and uncertainty in macromolecular free energy calculations. *J. Phys. Chem.* **1993**, *97*, 3409−3417.

(63) van der Zwan, G.; Hynes, J. Time dependent fluorescent solvent shifts, dielectric friction, and nonequilibrium solvation in polar solvents. *J. Phys. Chem.* **1985**, *89*, 4181−4188.

(64) Jimenez, R.; Fleming, G. R.; Kumar, P.; Maroncelli, M. Femtosecond solvation dynamics of water. *Nature* **1994**, *369*, 471−473.

(65) Chandler, D. *Introduction to modern statistical mechanics*; Oxford University Press: Oxford, U.K., 1987.

(66) Bader, J.; Chandler, D. Computer simulation of photochemically induced electron transfer. *Chem. Phys. Lett.* **1989**, *157*, 501−504.

(67) Thirumalai, D.; Berne, B. On the calculation of time correlation functions in quantum systems: path integral techniques. *J. Chem. Phys.* **1983**, *79*, 5029−5033.

(68) Allen, M.; Tildesley, D. *Computer Simulations of Liquids*; Clarendon Press: Oxford, U.K., 1991.

(69) Hall, R.; Berne, B. Nonergodicity in path integral molecular dynamics. *J. Chem. Phys.* **1984**, *81*, 3641−3643.

(70) Sun, M.; Song, P. *Photochem. Photobiol.* **1977**, *25*, 3.

(71) Meech, S.; Phillips, D.; Lee, A. *Chem. Phys.* **1983**, *80*, 317.

(72) Landau, L.; Lifschitz, E. *Statistical Mechanics*; Pergamon Press: New York, 1980.

(73) Simonson, T.; Perahia, D. Internal and interfacial dielectric properties of cytochrome c from molecular dynamics simulations in aqueous solution. *Proc. Natl. Acad Sci. U.S.A.* **1995**, *92*, 1082−1086.

(74) Simonson, T.; Perahia, D. Dielectric properties of proteins from simulations: tools and techniques. *Comput. Phys. Commun.* **1995**, *91*, 291−303.

(75) McClellan, A. *Tables of experimental dipole moments*; Freeman: London, 1963.